

Image Synthesis and Editing with Stochastic Differential Equations

Chenlin Meng¹ Yang Song¹ Jiaming Song¹
 Jiajun Wu¹ Jun-Yan Zhu² Stefano Ermon¹
¹Stanford University ²Carnegie Mellon University

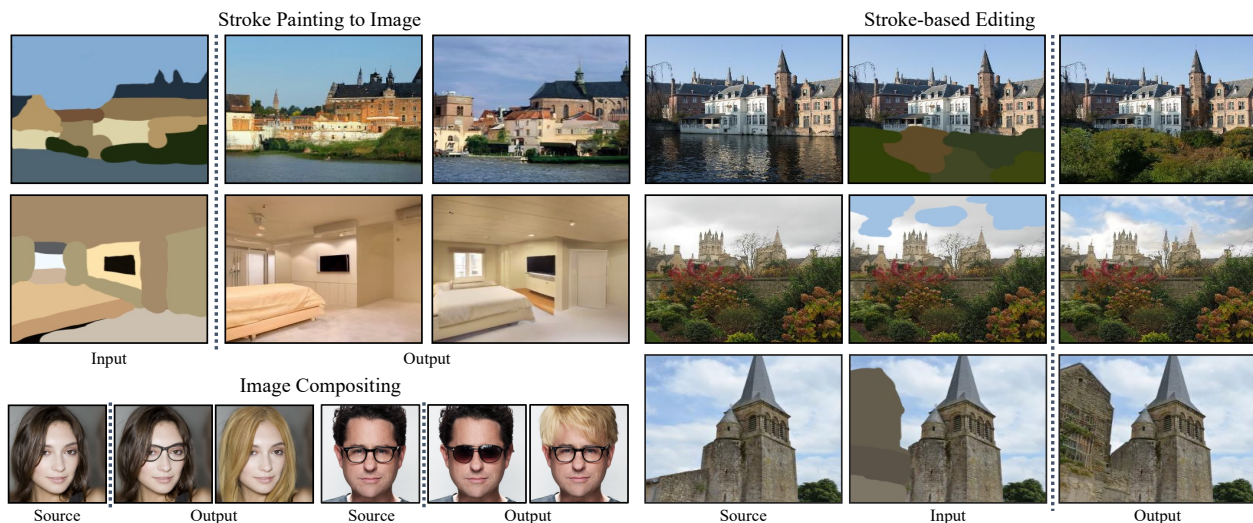


Figure 1: Stochastic Differential Editing (SDEdit) is a unified image synthesis and editing framework based on stochastic differential equations. SDEdit allows stroke painting to image, image compositing, and stroke-based editing without task-specific model training and loss functions.

Abstract

We introduce a new image editing and synthesis framework, *Stochastic Differential Editing (SDEdit)*, based on a recent generative model using stochastic differential equations (SDEs). Given an input image with user edits (e.g., hand-drawn color strokes), we first add noise to the input according to an SDE, and subsequently denoise it by simulating the reverse SDE to gradually increase its likelihood under the prior. Our method does not require task-specific loss function designs, which are critical components for recent image editing methods based on GAN inversion. Compared to conditional GANs, we do not need to collect new datasets of original and edited images for new applications. Therefore, our method can quickly adapt to various editing tasks at test time without re-training models. Our approach achieves strong performance on a wide range of applications, including image synthesis and editing guided by stroke paintings and image compositing.

1. Introduction

Denoising diffusion probabilistic models [23, 50] and score-based generative models [52, 55] are a new class of generative models that have found great success in image generation [52, 23, 53, 51, 55, 28, 13], audio synthesis [33] and graph generation [37]. One of the latest development in this direction, generative modeling with stochastic differential equations (SDEs [55]), has demonstrated comparable or better sample quality than generative adversarial networks (GANs) [17], with more stable training and better mode coverage. Specifically, Song et al. [55] proposed to perturb a data distribution according to the trajectory of an SDE by injecting Gaussian noise, which smoothly transforms any data distribution (e.g. images) to a tractable Gaussian prior distribution. To perform sampling, a neural network is trained to estimate the gradient of the data distribution, and subsequently uses it to solve the reverse stochastic process—a process that converts any Gaussian noise vector back to a data sample. Despite recent progress on uncondi-

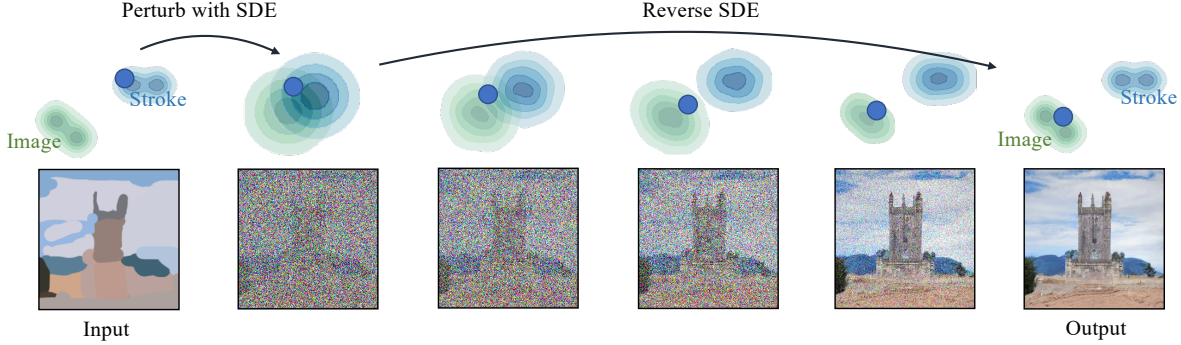


Figure 2: Synthesizing images from strokes with SDEdit. The blue dot illustrates the editing process of our method. The green and blue contour plots represent the distributions of images and stroke paintings, respectively. Given a stroke painting, we first perturb it by adding noise according to an SDE and progressively remove the noise by simulating the reverse SDE. This process gradually projects an unrealistic stroke painting to the manifold of natural images.

tional image generation, it remains challenging to use these models for real-world user-guided image synthesis and editing applications.

In this work, we propose Stochastic Differential Editing (SDEdit), a unified approach to image editing and synthesis inspired by generative modeling with stochastic differential equations (SDEs) [55]. The key intuition of SDEdit is to “hijack” the reverse stochastic process of SDE-based generative models, as illustrated in Fig. 2. Given an input image with user edits, such as a stroke painting or an image with strokes, we can add a suitable amount of noise to smooth out undesirable artifacts and distortions (*e.g.*, unnatural details at stroke pixels), while still preserving the overall structure of the input. We then initialize the reverse SDE with this noisy input, and simulate the reverse process to obtain a denoised result of high quality. Since both share the same noisy image, this denoised result and the user-edited input also share the overall image structure (see Fig. 2).

Existing methods for image editing are typically based on GANs, and can be roughly grouped into two categories. The first category leverages conditional GANs [26, 72] to learn a direct mapping from original images to edited ones. However, conditional models have to be trained on both original and edited images, thus requiring data collection and model re-training for new editing tasks. Unlike conditional GANs, SDEdit only requires training on the original image. As such, it can be directly applied to various editing tasks at test time (as illustrated in Figure 1).

The second category is GAN inversion [71, 9], where a pre-trained GAN is used to invert a given image to a latent representation, which is subsequently modified to generate the edited image. This procedure involves manually designing loss functions and optimization procedures for different image editing tasks. However, designing a proper loss function can be hard, and for tasks such as stroke-based image synthesis (Figure 1), no such loss exists in the literature. Moreover, many datasets are still hard to invert [32, 24] due to the limited model capacity and optimization difficulty.

Unlike GAN inversion, SDEdit does not solve an optimization problem, and is thus free of task-specific loss functions and optimization procedures. This makes our method especially advantageous when the loss function is hard to design (*e.g.*, stroke-based image synthesis in Figure 2).

We show that our unified framework enables several image synthesis and editing applications, including image compositing, stroke-based image synthesis, and stroke-based editing. Our empirical results confirm that SDEdit significantly outperforms GAN baselines on stroke-based image synthesis, with comparable performance on other tasks. We provide code and more details on our [website](#).

2. Related Work

Conditional GANs [26, 72] for image editing learn to directly generate an image based on a user input, and have demonstrated success on a variety of tasks including image synthesis and editing [42, 11, 12, 59, 39, 73], sketch2photo [47], inpainting [40, 25, 65, 35], photo colorization [67, 34, 68, 22], semantic image texture and geometry synthesis [69, 20, 61]. However, applying such methods to on-the-fly image manipulation is still challenging since a new model needs to be trained for each new application.

GANs Inversion and Editing. Another mainstream approach to image editing involves GAN inversion [71, 9], where the input is first projected into the latent space of an unconditional GAN before synthesizing a new image from the modified latent code. Several methods have been proposed in this direction, including fine-tuning network weights for each image [7, 38, 46], choosing better or multiple layers to project and edit [1, 2, 19, 60], designing better encoders [45, 57], modeling image corruption and transformations [5, 24], and discovering meaningful latent directions [49, 16, 27, 21]. However, these methods need to define different loss functions for different tasks. They

also require GAN inversion, which can be hard for certain datasets [24, 32, 8, 64].

Score-based Generative Models. Recent advances in training non-normalized probabilistic models, such as score-based generative models [52, 53, 55, 23, 51, 28] and energy-based models [3, 15, 14, 62, 63, 54], have achieved comparable image sample quality as GANs. However, most of the prior works in this direction have focused on unconditional image generation and density estimation, and state-of-the-art techniques for image editing and synthesis are still dominated by GAN-based methods. In this work, we focus on the recently emerged generative modeling with stochastic differential equations (SDE), and study its application to controllable image editing and synthesis tasks.

3. Background

Below we introduce the basic concepts of stochastic differential equations, and how to approximately reverse them by training neural networks.

3.1. Stochastic Differential Equations (SDEs)

Stochastic differential equations (SDEs) generalize ordinary differential equations (ODEs) by injecting random noise into the dynamics. The solution of an SDE is a time-varying random variable (*i.e.*, stochastic process), which we denote as $\mathbf{x}(t) \in \mathbb{R}^d$, where $t \in [0, 1]$ indexes time. The probability density function of $\mathbf{x}(t)$ is denoted as p_t .

We consider two special SDEs in this work: the Variance Exploding (VE) and Variance Preserving (VP) SDEs [55]. VE SDE gives a process with exploding variance, as used in [52, 53], while VP SDE yields a process with fixed variance of one under certain conditions, as used in [50, 23]. Though possessing slightly different forms and performing differently depending on the image domain, they share the same mathematical intuition. Since methods can be directly transferred from one to the other (and to other linear SDEs as well), we therefore only discuss the mathematical formulation of VE SDEs in the interest of space, and defer detailed information on VP SDEs to the appendix.

The VE SDE is given by

$$d\mathbf{x}(t) = \sqrt{\frac{d[\sigma^2(t)]}{dt}} d\mathbf{w}(t), \quad (1)$$

where $\sigma(t) \in \mathbb{R}$ is a pre-specified function that starts at $\sigma(0) = 0$ and grows exponentially fast. Here $d\mathbf{x}(t)$ represents the instantaneous increment of $\mathbf{x}(t)$, dt represents an infinitesimal time step, $\mathbf{w}(t) \in \mathbb{R}^d$ denotes a Brownian motion process, and $d\mathbf{w}(t)$ stands for an infinitesimal difference of $\mathbf{w}(t)$ which can be intuitively understood as infinitesimal Gaussian noise.

For VE SDEs, $\mathbf{x}(t)$ is always distributed according to a Gaussian centered at $\mathbf{x}(0)$. Specifically,

$$p(\mathbf{x}(t) | \mathbf{x}(0)) = \mathcal{N}(\mathbf{x}(t) | \mathbf{x}(0), \sigma^2(t)\mathbf{I}).$$

Intuitively, the stochastic process perturbs $\mathbf{x}(0)$ with increasing Gaussian noise as time moves forward, which makes obtaining $\mathbf{x}(t)$ from $\mathbf{x}(0)$ particularly easy. Under the condition that $\sigma(1)$ is sufficiently large, $\mathbf{x}(1)$ will be approximately distributed according to $\mathcal{N}(\mathbf{0}, \sigma^2(1)\mathbf{I})$ regardless of the value of $\mathbf{x}(0)$, *i.e.*, $p_1 \approx \mathcal{N}(\mathbf{0}, \sigma^2(1)\mathbf{I})$.

3.2. Reversing SDEs

As time elapses, the SDE progressively adds Gaussian noise to $\mathbf{x}(0)$. By reversing this process, we can gradually denoise $\mathbf{x}(t)$ to recover $\mathbf{x}(0)$. [4] shows that any SDE has a corresponding reverse SDE that depends on $\nabla_{\mathbf{x}} \log p_t(\mathbf{x})$, a quantity commonly known as the (*Stein*) *score function* [56, 36, 18] of $p_t(\mathbf{x})$. In particular, the reverse VE SDE is

$$d\mathbf{x}(t) = \frac{d[\sigma^2(t)]}{dt} \nabla_{\mathbf{x}} \log p_t(\mathbf{x}(t)) dt + \sqrt{\frac{d[\sigma^2(t)]}{dt}} d\bar{\mathbf{w}}(t). \quad (2)$$

where dt here is an infinitesimal negative time step, p_t denotes the distribution of $\mathbf{x}(t)$, and $\bar{\mathbf{w}}(t) \in \mathbb{R}^d$ is a Brownian motion running backwards in time. Both forward and reverse SDEs induce the same stochastic process $\{\mathbf{x}(t)\}_{t \in [0, 1]}$, except that time progresses in the reverse direction for the reverse SDE.

To obtain the reverse SDE, it is necessary to know the score function $\nabla_{\mathbf{x}} \log p_t(\mathbf{x}(t))$ for all $t \in [0, 1]$. Suppose the initial distribution of the SDE, p_0 , is chosen to be the underlying data distribution of a dataset. We can estimate these score functions by training a time-dependent neural network $\mathbf{s}_{\theta}(\cdot, t) : \mathbb{R}^d \rightarrow \mathbb{R}^d$, called a *time-dependent score model*, on this dataset such that $\mathbf{s}_{\theta}(\mathbf{x}, t) \approx \nabla_{\mathbf{x}} \log p_t(\mathbf{x})$.

The training objective for $\mathbf{s}_{\theta}(\mathbf{x}, t)$ is a mixture of denoising score matching losses [58, 44, 43] over randomly sampled time steps. For VE SDEs, it takes the form of

$$\min_{\theta} \mathbb{E}_{t \sim \mathcal{U}(0, 1)} \mathbb{E}_{\mathbf{x}(0) \sim p_0} \mathbb{E}_{\mathbf{x}(t) \sim \mathcal{N}(\mathbf{x}(0), \sigma^2(t)\mathbf{I})} \left[\left\| \sigma(t) \mathbf{s}_{\theta}(\mathbf{x}(t), t) + \frac{\mathbf{x}(t) - \mathbf{x}(0)}{\sigma(t)} \right\|_2^2 \right]. \quad (3)$$

Here all expectations can be estimated with empirical means over samples. Intuitively, the objective pushes $\mathbf{s}_{\theta}(\mathbf{x}(t), t)$ to recover the Gaussian noise that perturbed $\mathbf{x}(0)$ to $\mathbf{x}(t)$, and the resulting score model can be interpreted as a denoiser for $\mathbf{x}(t)$. We can minimize the objective with standard Stochastic Gradient Descent, with no need for adversarial training.

With the learned time-dependent score model in hand, we can plug it into the reverse SDE. This allows us to

gradually transform a Gaussian noise vector $\mathbf{x}(1) \sim p_1 \approx \mathcal{N}(\mathbf{0}, \sigma^1(1)\mathbf{I})$ to a data sample $\mathbf{x}(0) \sim p_0$. Following previous work [55], we solve the reverse VE and VP SDEs by discretizing the time interval, where $[0, 1]$ is uniformly partitioned to N equal sub-intervals, with end points $0 = t_0 < t_1 < \dots < t_N = 1$ and $\Delta t = \frac{1}{N}$. In particular, we solve the reverse VE SDE by iterating

$$\mathbf{x}_{n-1} = \mathbf{x}_n + (\sigma^2(t_n) - \sigma^2(t_n - \Delta t))\mathbf{s}_\theta(\mathbf{x}_n, t_n) + \sqrt{\sigma^2(t_n) - \sigma^2(t_n - \Delta t)}\mathbf{z}_n, \quad (4)$$

where $n \in \{1, 2, \dots, N\}$, $\mathbf{x}_N \sim \mathcal{N}(\mathbf{0}, \sigma^2(1)\mathbf{I})$ and $\mathbf{z}_n \sim \mathcal{N}(\mathbf{0}, \mathbf{I})$. When $\Delta t \approx 0$, we have $\sigma^2(t) - \sigma^2(t - \Delta t) \approx \frac{d[\sigma^2(t)]}{dt} \Delta t$, making Eq. (4) close to Eq. (2). As a result, the sequence of random variables $\{\mathbf{x}_n\}_{n=0}^N$ obtained from Eq. (4) becomes an approximation of the stochastic process $\{\mathbf{x}(t)\}_{t \in [0, 1]}$ (i.e., $\mathbf{x}_n \approx \mathbf{x}(t_n) \sim p_{t_n}$ for each n). Note that Eq. (4) is only one numerical integration scheme, and other numerical SDE solvers [48] also work. Reversing VP SDEs can be similarly achieved with a uniform discretization and the time-dependent score model, which we defer to the appendix.

4. Image Synthesis and Editing with SDEs

Leveraging SDEs and their reverse, we propose a unified approach for multiple tasks in image synthesis and editing, including stroke-based image synthesis, stroke-based image editing and image compositing as shown in Fig. 1. For each image domain, we only need to train a single time-dependent score model to build a prior for performing all these tasks. We call our method *Stochastic Differential Editing (SDEdit)*. As we shall see later, SDEdit does not require task-specific model training or loss function designs, and is advantageous when the loss function for GAN-based methods is hard to design (e.g., stroke-based image synthesis in Figure 2). Moreover, SDEdit does not require training on paired or unpaired edited images, and is directly applicable to various image editing and synthesis tasks.

4.1. Training the Score Model

Before performing various editing tasks, we need a dataset of images that captures the prior of a particular image domain. For example, we need a dataset of diverse human faces for performing face editing, and a dataset of high quality bedrooms for synthesizing bedroom images.

Suppose the dataset contains M images, denoted as $\{\mathbf{x}^{(1)}, \mathbf{x}^{(2)}, \dots, \mathbf{x}^{(M)}\}$, which are i.i.d. sampled from an underlying data distribution p_{data} . As a first step of our method, we perturb the training data with an SDE by setting $p_0 = p_{\text{data}}$, and train a time-dependent score model $\mathbf{s}_\theta(\mathbf{x}(t), t)$ to denoise perturbed samples by optimizing Eq. (3).

4.2. Synthesizing Images from Strokes

With the learned time-dependent score model $\mathbf{s}_\theta(\mathbf{x}(t), t)$ at our disposal, we can synthesize and edit images in the same domain without re-training models. We first introduce a simplified version of our algorithm before discussing the general case. Let us consider the task of stroke-based image synthesis, where we aim to generate photo-realistic images guided by strokes from a user (see Fig. 2). The stroke painting describes the rough content in a target image with color blocks, and we aim to infer high quality images from our prior while preserving semantics of the stroke painting. Compared to Scribber [47], our stroke paintings only require rough color strokes and do not rely on detailed sketches, which are hard for novice users to create.

Generating images from strokes is challenging for GAN inversion methods due to the difficulty of designing a suitable loss to measure the difference between strokes and images, as the loss should assess semantic similarity instead of pixel-wise distances. Solving this task with SDEs, however, is rather straightforward as we observe that the distributions of strokes and images can be smoothly bridged together by adding large Gaussian noise. As illustrated in Fig. 2, we can first perturb an input stroke according to the SDE until it loses details but not general structure. Subsequently, we denoise the noisy stroke to progressively move it to the distribution of valid images captured by the time-dependent score model.

This intuition can be implemented with the reverse SDE and a pre-trained time-dependent score model. We first start with a stroke painting $\mathbf{x}(0)$ and run the forward SDE until $t = t_0$ to obtain $\mathbf{x}(t_0)$, where $0 < t_0 < 1$ is a hyper-parameter tuned such that $\mathbf{x}(t_0)$ blurs the unrealistic details in $\mathbf{x}(0)$ without significantly altering its global semantics and structure. We then reverse the stochastic process with the time-dependent score model using the numerical procedure given in Eq. (4). Because the forward and reverse processes are stochastic, we do not recover the original stroke painting, but instead obtain a modified image steered towards the prior distribution of valid images, on which our score-based models have been trained. We can repeat the above perturbing and denoising procedure for this modified image, in order to move it closer to the data distribution for improved fidelity. The pseudo-code is given in Algorithm 1 for the VE SDE, where N denotes the number of denoising steps, and K is the number of total repeats.

4.3. SDEdit: General Algorithm

Algorithm 1 converts a stroke painting to a photo-realistic image, which typically modifies all pixels of the input. However, in cases such as image compositing and stroke-based editing, certain regions of the input are already photo-realistic and therefore we hope to leave these regions intact. To represent a specific region, we use a binary mask

Algorithm 1 Stroke-based image synthesis with SDEdit

Require: \mathbf{x} (stroke painting), t_0 (SDE hyper-parameter), N (total denoising steps), K (total repeats)

$$\Delta t \leftarrow \frac{t_0}{N}$$

for $k \leftarrow 1$ **to** K **do**

$$\mathbf{z} \sim \mathcal{N}(\mathbf{0}, \mathbf{I})$$

$$\mathbf{x} \leftarrow \mathbf{x} + \sigma(t_0)\mathbf{z}$$

for $n \leftarrow N$ **to** 1 **do**

$$t \leftarrow t_0 \frac{n}{N}$$

$$\mathbf{z} \sim \mathcal{N}(\mathbf{0}, \mathbf{I})$$

$$\epsilon \leftarrow \sqrt{\sigma^2(t) - \sigma^2(t - \Delta t)}$$

$$\mathbf{x} \leftarrow \mathbf{x} + \epsilon s_\theta(\mathbf{x}, t) + \epsilon \mathbf{z}$$

end for

end for

Return \mathbf{x}

$\Omega \in \{0, 1\}^{C \times H \times W}$ that evaluates to 1 for editable pixels and 0 otherwise. We can generalize Algorithm 1 to restrict editing in the region defined by Ω .

For editable regions, we perturb the input image with the forward SDE and generate edits by reversing the SDE, using the same procedure in Algorithm 1. For uneditable regions, we perturb it as usual but design the reverse procedure carefully so that it is guaranteed to recover the input. Specifically, suppose $\mathbf{x} \in \mathbb{R}^{C \times H \times W}$ is an input image of height H , width W , and with C channels. Our algorithm first perturbs $\mathbf{x}(0) = \mathbf{x}$ with an SDE running from $t = 0$ till $t = t_0$ to obtain $\mathbf{x}(t_0)$, where $0 < t_0 \leq 1$ is a hyper-parameter tuned in the same way as Section 4.2. Afterwards, we denoise $\mathbf{x}(t_0)$ with separate methods for $\Omega \odot \mathbf{x}(t)$ and $(1 - \Omega) \odot \mathbf{x}(t)$, where \odot denotes the element-wise product and $0 \leq t \leq t_0$. For $\Omega \odot \mathbf{x}(t)$, we simulate the reverse SDE in Eq. (2) and project the results by element-wise multiplication with Ω . For $(1 - \Omega) \odot \mathbf{x}(t)$, we set it to $(1 - \Omega) \odot (\mathbf{x} + \sigma(t)\mathbf{z})$, where $\mathbf{z} \sim \mathcal{N}(\mathbf{0}, \mathbf{I})$. Here we gradually reduce the noise magnitude according to $\sigma(t)$ to make sure $\Omega \odot \mathbf{x}(t)$ and $(1 - \Omega) \odot \mathbf{x}(t)$ have comparable amount of noise. Moreover, since $\sigma(t) \rightarrow 0$ as $t \rightarrow 0$, this ensures that $(1 - \Omega) \odot \mathbf{x}(t)$ converges to $(1 - \Omega) \odot \mathbf{x}$, keeping the uneditable part of \mathbf{x} intact. The complete SDEdit method (for VE SDEs) is given in Algorithm 2, and we provide additional pseudo-code for VP SDEs in the supplementary material.

With different inputs to Algorithm 2, we can perform multiple image synthesis and editing tasks with a single unified approach, including but not limited to the following:

- **Stroke-based image synthesis:** We can recover Algorithm 1 discussed in Section 4.2 by setting all entries in Ω to 1.
- **Stroke-based image editing:** Suppose \mathbf{x} is an image marked by strokes, and Ω masks the part of stroke painting. We can reconcile the two parts of \mathbf{x} with

Algorithm 2 Stochastic Differential Editing (VE SDE)

Require: \mathbf{x} (raw image), Ω (mask for edited regions), t_0 (SDE hyper-parameter), N (total denoising steps), K (total repeats)

$$\Delta t \leftarrow \frac{t_0}{N}$$

$$\mathbf{x}_0 \leftarrow \mathbf{x}$$

for $k \leftarrow 1$ **to** K **do**

$$\mathbf{z} \sim \mathcal{N}(\mathbf{0}, \mathbf{I})$$

$$\mathbf{x} \leftarrow (1 - \Omega) \odot \mathbf{x}_0 + \Omega \odot \mathbf{x} + \sigma(t_0)\mathbf{z}$$

for $n \leftarrow N$ **to** 1 **do**

$$t \leftarrow t_0 \frac{n}{N}$$

$$\mathbf{z} \sim \mathcal{N}(\mathbf{0}, \mathbf{I})$$

$$\epsilon \leftarrow \sqrt{\sigma^2(t) - \sigma^2(t - \Delta t)}$$

$$\mathbf{x} \leftarrow (1 - \Omega) \odot (\mathbf{x}_0 + \sigma(t)\mathbf{z}) + \Omega \odot (\mathbf{x} + \epsilon s_\theta(\mathbf{x}, t) + \epsilon \mathbf{z})$$

end for

end for

Return \mathbf{x}

	% more faithful than SDEdit (VE)(1) \uparrow	% more realistic than SDEdit (VE)(1) \uparrow
in-domain GAN-1 [70]	13.55%	11.93%
in-domain GAN-2 [70]	13.27%	8.72%
StyleGAN2-ADA [30]	8.94%	5.88%
SDEdit (VE) (1) (ours)	—	—
SDEdit (VE) (3) (ours)	52.53%	60.66%
SDEdit (VP) (1) (ours)	61.34%	60.59%
SDEdit (VP) (3) (ours)	68.50%	73.58%

Table 1: Evaluation of stroke-based generation on LSUN bedroom dataset. The parenthesis after SDEdit (VP/VE) indicates the number of repetitions k . Numbers are the percentage of MTurk workers that prefers a method over our SDEdit (VE) (1).

Algorithm 2 to obtain a photo-realistic image.

- **Image compositing:** Suppose \mathbf{x} is an image superimposed by elements from two images, and Ω masks the region belonging to the same image. We can perform image compositing with Algorithm 2.

5. Experiments

We show that SDEdit is able to outperform state-of-the-art GAN models on stroke-based image synthesis, and achieves competitive performance on stroke-based image editing, and image compositing. Both the baselines and our SDEdit use pre-trained models that are publicly available.

5.1. Stroke-Based Image Synthesis

Given an input stroke painting, our goal is to generate a realistic image that shares the same structure as the input *when no paired data is available*. We present the results of SDEdit using both VE and VP SDEs in Figure 3. We consider $K = 1$ and $K = 3$ to compare and contrast the per-

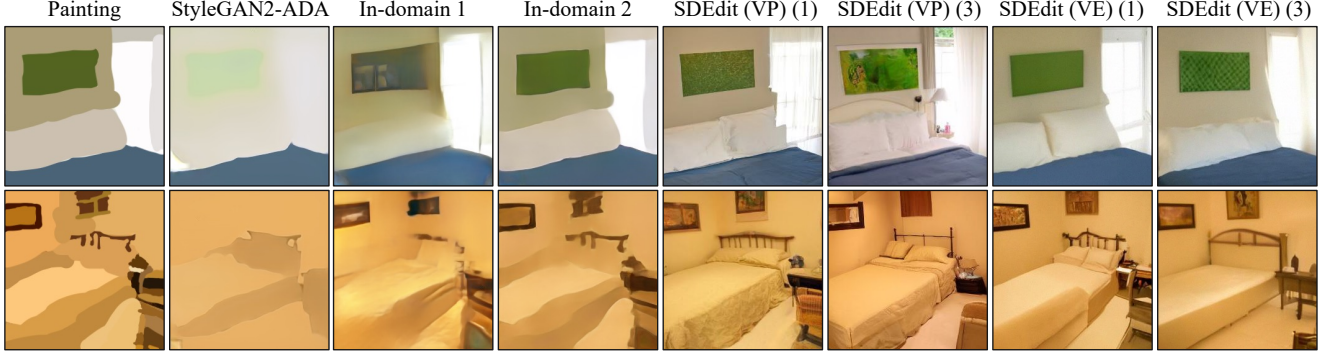


Figure 3: Generated images based on stroke paintings on LSUN bedroom dataset. We generated 400 images for each method. We compare our results with StyleGAN2-ADA and in-domain GAN. In the figure, the parenthesis after SDEdit (VP/VE) stands for the number of iterations used.

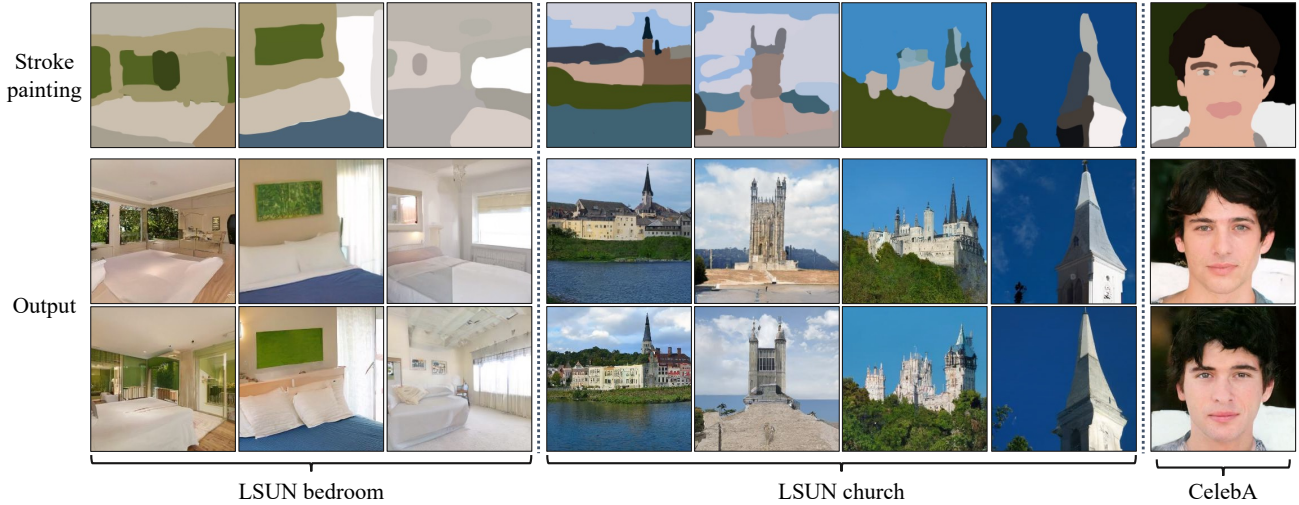


Figure 4: Stroke-based image synthesis with SDEdit (VP) on LSUN bedroom, LSUN church and CelebA-HQ (256×256) datasets. We notice that SDEdit is able to generated multiple diverse images for each stroke painting.

formance of different number of repetitions in Algorithm 1. More detailed settings are given in the appendix.

For comparison, we choose two representative GAN-based methods on image editing and synthesis as our baselines. Our first baseline is the image projection method used in StyleGAN2-ADA [30], where inversion is done in the W^+ space of StyleGANs by minimizing the perceptual loss. Our second baseline is in-domain GAN [70], where inversion is accomplished by running optimization steps on top of an encoder. Specifically, we consider two versions of the in-domain GAN inversion techniques: the first one (denoted as In-domain 1) only uses the encoder to maximize the inversion speed, whereas the second (denoted as In-domain 2) runs additional optimization steps to maximize the inversion accuracy. We present more details on baseline models in the appendix.

As Figure 3 demonstrates, both baselines struggle to generate realistic images based on stroke painting inputs whereas our method successfully generates realistic images that preserve semantics of the input stroke painting. In addition, as shown in Figure 4, our SDEdit can synthesize diverse images for the same input.

We leverage Amazon Mechanical Turk to quantify the advantage of our SDEdit over baselines. Specifically, we synthesize a total of 400 bedroom images from stroke paintings for each method. To quantify sample quality, we ask the workers to perform 1500 pairwise comparisons (against SDEdit (VE) ($k = 1$)) to determine which image sample looks more realistic. To quantify faithfulness (*i.e.* whether synthesized samples preserve semantics of the stroke painting), we ask a different set of workers to perform another 3000 pairwise comparisons (against SDEdit (VE) ($k = 1$)).

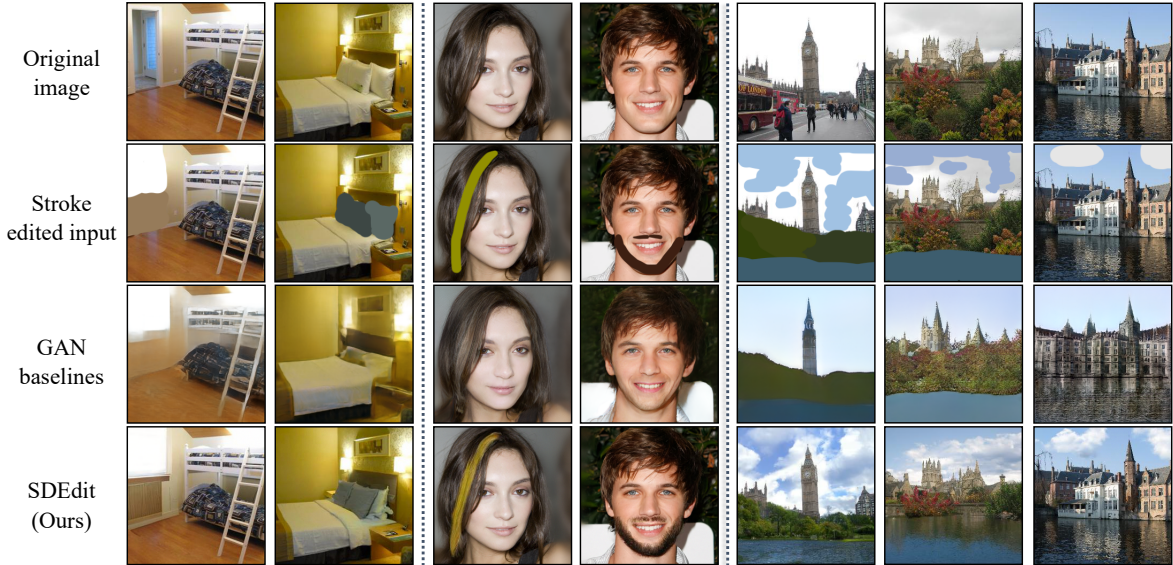


Figure 5: Stroke-based image editing with SDEdit (VP) on LSUN bedroom, CelebA-HQ, and LSUN church datasets. For comparison, we also show the results of GAN baselines with the same inputs, where results for LSUN bedroom and CelebA-HQ are obtained by in-domain GAN (the first 4 panels), and results for LSUN church are from StyleGAN2-ADA (the rightmost 3 panels). We observe that our method is able to generate images that are more faithful and realistic compared to the baselines.

All quantitative results for this task are given in Table 1. We observe that all the SDEdit methods are able to beat the GAN baselines on both faithfulness and sample quality, with SDEdit (VP) ($k = 3$) achieving the best performance.

5.2. Flexible Image Editing

With the same pre-trained time-dependent score models, we can perform a variety of different image editing tasks with Algorithm 2. We focus on LSUN (bedroom, church) and CelebA-HQ datasets, and provide more details on the experimental setup in the appendix.

5.2.1 Stroke-based image editing

We ask users to add stroke edits to real images, and then specify the masks to describe the locations of the strokes. Similar to our previous experiments, we use StyleGAN-ADA and in-domain GAN as our baselines. We feed the same scribbled images to all the models. As shown in Figure 5, results generated by GAN baselines tend to introduce undesired modifications, occasionally making the image outside the stroke region blurry. In contrast, our method is able to generate image edits that are both realistic and faithful (to the user edit), while avoid making undesired modifications.

5.2.2 Image compositing

We focus on compositing images from the CelebA-HQ [29] dataset. Given an image randomly sampled from the dataset, we ask the users to specify how they want the edited image to look like using pixel patches copied from other reference images (examples in Figure 6 where “original” stands for a dataset image, and “input” for an input designed by users). We ask users to specify the pixels they want to perform modifications, which will be used as the mask in Algorithm 2. We compare our method to traditional blending algorithms and the same GAN baselines considered previously. We present the results in Figure 6 where we use the same input for all the methods. To quantitatively evaluate our results, we generate 936 images based on the user inputs. To quantify sample quality, we ask MTurk workers to perform 1500 pairwise comparisons (against SDEdit (VE) pre-trained on FFHQ [31]) to determine which image sample looks more realistic. To quantify faithfulness (*i.e.* whether the generated images follows the user’s edit), we ask different workers to perform another 1500 pairwise comparisons (against SDEdit (VE) pre-trained on FFHQ) to decide which generated image matches the content of the inputs more faithfully. To quantify undesired changes, we follow [6] to compute masked LPIPS [66]. As evidenced in Table 2, we observe that SDEdit is able to generate both faithful and realistic images with much lower LPIPS scores compared to GAN baselines. We present more experiment

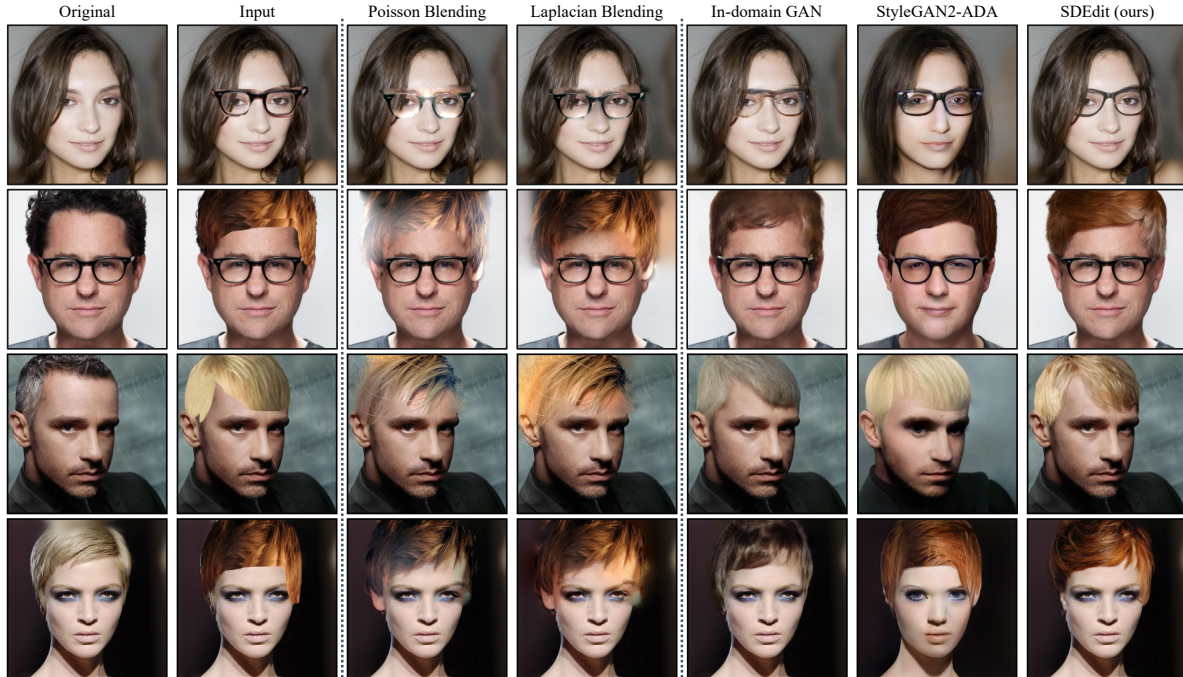


Figure 6: Image editing on CelebA with models trained on FFHQ. Given an input image, we use the same mask for all methods. Quantitative results are reported in Table 2

	% more faithful than SDEdit (VE) (FFHQ) \uparrow	% more realistic than SDEdit (VE) (FFHQ) \uparrow	LPIPS (masked) \downarrow
Laplacian Blending [10]	16.27%	24.73%	0.09
Poisson Blending [41]	17.82%	24.40%	0.05
in-domain GAN [70]	26.47%	46.92%	0.23
StyleGAN2-ADA [30]	16.57%	25.88%	0.21
SDEdit (VE) (FFHQ) (ours)	—	—	0.03
SDEdit (VE) (CelebA) (ours)	57.23%	49.54%	0.03
SDEdit (VP) (CelebA) (ours)	41.80%	49.26%	0.07

Table 2: Image editing on CelebA-HQ images. All the GAN baselines are trained on FFHQ [31]. For SDEdit, we denote in the parenthesis which dataset it is pre-trained on. Numbers indicate the percentage of MTurk workers that prefer the corresponding method over SDEdit (VE) (FFHQ). We report the masked LPIPS distance between edited and unchanged images to quantify undesired changes outside the masks.

settings in the appendix.

6. Conclusion

We propose Stochastic Differential Editing (SDEdit), an image editing and synthesis method via generative modeling of images with stochastic differential equations (SDEs). Unlike image editing techniques via GAN inversion, our method does not require task-specific optimization algorithms for reconstructing inputs, and is particularly suitable for datasets or tasks where GAN inversion losses are hard to design or optimize. We demonstrate that SDEdit outper-

forms existing GAN-based methods on stroke-based image generation, and also achieves competitive performance on stroke-based image editing and image compositing with no or minor modifications.

Acknowledgments. The authors want to thank Kristy Choi for proofreading. This research was supported by NSF (#1651565, #1522054, #1733686), ONR (N00014-19-1-2145), AFOSR (FA9550-19-1-0024), ARO, Autodesk, Stanford HAI, Amazon ARA, and Amazon AWS. Yang Song is supported by the Apple PhD Fellowship in AI/ML. J.-Y. Zhu is partly supported by Naver Corporation.

References

- [1] Rameen Abdal, Yipeng Qin, and Peter Wonka. Image2stylegan: How to embed images into the stylegan latent space? In *Proceedings of the IEEE/CVF International Conference on Computer Vision*, pages 4432–4441, 2019.
- [2] Rameen Abdal, Yipeng Qin, and Peter Wonka. Image2stylegan++: How to edit the embedded images? In *Proceedings of the IEEE/CVF Conference on Computer Vision and Pattern Recognition*, pages 8296–8305, 2020.
- [3] David H Ackley, Geoffrey E Hinton, and Terrence J Sejnowski. A learning algorithm for boltzmann machines. *Cognitive science*, 9(1):147–169, 1985.
- [4] Brian DO Anderson. Reverse-time diffusion equation models. *Stochastic Processes and their Applications*, 12(3):313–326, 1982.
- [5] Rushil Anirudh, Jayaraman J Thiagarajan, Bhavya Kaikhura, and Peer-Timo Bremer. Mimicgan: Robust projection onto image manifolds with corruption mimicking. *International Journal of Computer Vision*, pages 1–19, 2020.
- [6] David Bau, Steven Liu, Tongzhou Wang, Jun-Yan Zhu, and Antonio Torralba. Rewriting a deep generative model. In *European Conference on Computer Vision (ECCV)*, 2020.
- [7] David Bau, Hendrik Strobelt, William Peebles, Jonas Wulff, Bolei Zhou, Jun-Yan Zhu, and Antonio Torralba. Semantic photo manipulation with a generative image prior. *ACM SIGGRAPH*, 38(4):1–11, 2019.
- [8] David Bau, Jun-Yan Zhu, Jonas Wulff, William Peebles, Hendrik Strobelt, Bolei Zhou, and Antonio Torralba. Seeing what a gan cannot generate. In *Proceedings of the IEEE/CVF International Conference on Computer Vision*, pages 4502–4511, 2019.
- [9] Andrew Brock, Theodore Lim, James M Ritchie, and Nick Weston. Neural photo editing with introspective adversarial networks. In *International Conference on Learning Representations (ICLR)*, 2017.
- [10] Peter J Burt and Edward H Adelson. The laplacian pyramid as a compact image code. In *Readings in computer vision*, pages 671–679. Elsevier, 1987.
- [11] Qifeng Chen and Vladlen Koltun. Photographic image synthesis with cascaded refinement networks. In *IEEE International Conference on Computer Vision (ICCV)*, 2017.
- [12] Tali Dekel, Chuhan Gan, Dilip Krishnan, Ce Liu, and William T Freeman. Sparse, smart contours to represent and edit images. In *IEEE Conference on Computer Vision and Pattern Recognition (CVPR)*, 2018.
- [13] Prafulla Dhariwal and Alex Nichol. Diffusion models beat gans on image synthesis. *arXiv preprint arXiv:2105.05233*, 2021.
- [14] Yilun Du and Igor Mordatch. Implicit generation and generalization in energy-based models. *arXiv preprint arXiv:1903.08689*, 2019.
- [15] Ruiqi Gao, Yang Lu, Junpei Zhou, Song-Chun Zhu, and Ying Nian Wu. Learning energy-based models as generative convnets via multi-grid modeling and sampling. *arXiv e-prints*, pages arXiv–1709, 2017.
- [16] Lore Goetschalckx, Alex Andonian, Aude Oliva, and Phillip Isola. Ganalyze: Toward visual definitions of cognitive image properties. In *IEEE International Conference on Computer Vision (ICCV)*, 2019.
- [17] Ian J Goodfellow, Jean Pouget-Abadie, Mehdi Mirza, Bing Xu, David Warde-Farley, Sherjil Ozair, Aaron Courville, and Yoshua Bengio. Generative adversarial networks. *arXiv preprint arXiv:1406.2661*, 2014.
- [18] Jackson Gorham and Lester Mackey. Measuring sample quality with stein’s method. *arXiv preprint arXiv:1506.03039*, 2015.
- [19] Jinjin Gu, Yujun Shen, and Bolei Zhou. Image processing using multi-code gan prior. In *IEEE Conference on Computer Vision and Pattern Recognition (CVPR)*, 2020.
- [20] Éric Guérin, Julie Digne, Éric Galin, Adrien Peytavie, Christian Wolf, Bedrich Benes, and Benoufdefinedt Martinez. Interactive example-based terrain authoring with conditional generative adversarial networks. *ACM Transactions on Graphics (TOG)*, 36(6), 2017.
- [21] Erik Härkönen, Aaron Hertzmann, Jaakko Lehtinen, and Sylvain Paris. Ganspace: Discovering interpretable gan controls. In *Advances in Neural Information Processing Systems*, 2020.
- [22] Mingming He, Dongdong Chen, Jing Liao, Pedro V Sander, and Lu Yuan. Deep exemplar-based colorization. *ACM Transactions on Graphics (TOG)*, 37(4):1–16, 2018.
- [23] Jonathan Ho, Ajay Jain, and Pieter Abbeel. Denoising diffusion probabilistic models. *arXiv preprint arXiv:2006.11239*, 2020.
- [24] Minyoung Huh, Richard Zhang, Jun-Yan Zhu, Sylvain Paris, and Aaron Hertzmann. Transforming and projecting images into class-conditional generative networks. In *European Conference on Computer Vision (ECCV)*, 2020.
- [25] Satoshi Iizuka, Edgar Simo-Serra, and Hiroshi Ishikawa. Globally and locally consistent image completion. *ACM Transactions on Graphics (TOG)*, 36(4):107, 2017.
- [26] Phillip Isola, Jun-Yan Zhu, Tinghui Zhou, and Alexei A Efros. Image-to-image translation with conditional adversarial networks. In *IEEE Conference on Computer Vision and Pattern Recognition (CVPR)*, 2017.
- [27] Ali Jahanian, Lucy Chai, and Phillip Isola. On the “steerability” of generative adversarial networks. In *International Conference on Learning Representations (ICLR)*, 2020.
- [28] Alexia Jolicœur-Martineau, Rémi Piché-Taillefer, Ioannis Mitliagkas, and Remi Tachet des Combes. Adversarial score matching and improved sampling for image generation. In *International Conference on Learning Representations*, 2021.
- [29] Tero Karras, Timo Aila, Samuli Laine, and Jaakko Lehtinen. Progressive growing of gans for improved quality, stability, and variation. *arXiv preprint arXiv:1710.10196*, 2017.
- [30] Tero Karras, Miika Aittala, Janne Hellsten, Samuli Laine, Jaakko Lehtinen, and Timo Aila. Training generative adversarial networks with limited data. *arXiv preprint arXiv:2006.06676*, 2020.

- [31] Tero Karras, Samuli Laine, and Timo Aila. A style-based generator architecture for generative adversarial networks. In *IEEE Conference on Computer Vision and Pattern Recognition (CVPR)*, 2019.
- [32] Tero Karras, Samuli Laine, Miika Aittala, Janne Hellsten, Jaakko Lehtinen, and Timo Aila. Analyzing and improving the image quality of stylegan. In *IEEE Conference on Computer Vision and Pattern Recognition (CVPR)*, 2020.
- [33] Zhifeng Kong, Wei Ping, Jiaji Huang, Kexin Zhao, and Bryan Catanzaro. Diffwave: A versatile diffusion model for audio synthesis. In *International Conference on Learning Representations (ICLR)*, 2020.
- [34] Gustav Larsson, Michael Maire, and Gregory Shakhnarovich. Learning representations for automatic colorization. In *European Conference on Computer Vision (ECCV)*, 2016.
- [35] Guilin Liu, Fitsum A Reda, Kevin J Shih, Ting-Chun Wang, Andrew Tao, and Bryan Catanzaro. Image inpainting for irregular holes using partial convolutions. In *European Conference on Computer Vision (ECCV)*, 2018.
- [36] Qiang Liu, Jason Lee, and Michael Jordan. A kernelized stein discrepancy for goodness-of-fit tests. In *International conference on machine learning*, pages 276–284. PMLR, 2016.
- [37] Chenhao Niu, Yang Song, Jiaming Song, Shengjia Zhao, Aditya Grover, and Stefano Ermon. Permutation invariant graph generation via score-based generative modeling. In *International Conference on Artificial Intelligence and Statistics*, pages 4474–4484. PMLR, 2020.
- [38] Xingang Pan, Xiaohang Zhan, Bo Dai, Dahua Lin, Chen Change Loy, and Ping Luo. Exploiting deep generative prior for versatile image restoration and manipulation. In *European Conference on Computer Vision*, 2020.
- [39] Taesung Park, Ming-Yu Liu, Ting-Chun Wang, and Jun-Yan Zhu. Semantic image synthesis with spatially-adaptive normalization. In *IEEE Conference on Computer Vision and Pattern Recognition (CVPR)*, 2019.
- [40] Deepak Pathak, Philipp Krahenbuhl, Jeff Donahue, Trevor Darrell, and Alexei A Efros. Context encoders: Feature learning by inpainting. In *IEEE Conference on Computer Vision and Pattern Recognition (CVPR)*, 2016.
- [41] Patrick Pérez, Michel Gangnet, and Andrew Blake. Poisson image editing. In *ACM SIGGRAPH*, pages 313–318, 2003.
- [42] Tiziano Portenier, Qiyang Hu, Attila Szabó, Siavash Arjomand Bigdeli, Paolo Favaro, and Matthias Zwicker. Faceshop: Deep sketch-based face image editing. *ACM Transactions on Graphics (TOG)*, 37(4), 2018.
- [43] Martin Raphan and Eero P Simoncelli. Least squares estimation without priors or supervision. *Neural computation*, 23(2):374–420, 2011.
- [44] Martin Raphan, Eero P Simoncelli, B Scholkopf, J Platt, and T Hoffman. Learning to be bayesian without supervision. *Advances in neural information processing systems*, 19:1145, 2007.
- [45] Elad Richardson, Yuval Alaluf, Or Patashnik, Yotam Nitzan, Yaniv Azar, Stav Shapiro, and Daniel Cohen-Or. Encoding in style: a stylegan encoder for image-to-image translation. In *Proceedings of the IEEE/CVF Conference on Computer Vision and Pattern Recognition*, 2021.
- [46] Daniel Roich, Ron Mokady, Amit H Bermano, and Daniel Cohen-Or. Pivotal tuning for latent-based editing of real images. *arXiv preprint arXiv:2106.05744*, 2021.
- [47] Patsorn Sangkloy, Jingwan Lu, Chen Fang, Fisher Yu, and James Hays. Scribbler: Controlling deep image synthesis with sketch and color. In *IEEE Conference on Computer Vision and Pattern Recognition (CVPR)*, 2017.
- [48] Timothy Sauer. Numerical solution of stochastic differential equations in finance. In *Handbook of computational finance*, pages 529–550. Springer, 2012.
- [49] Yujun Shen, Jinjin Gu, Xiaoou Tang, and Bolei Zhou. Interpreting the latent space of gans for semantic face editing. In *IEEE Conference on Computer Vision and Pattern Recognition (CVPR)*, 2020.
- [50] Jascha Sohl-Dickstein, Eric A Weiss, Niru Maheswaranathan, and Surya Ganguli. Deep unsupervised learning using nonequilibrium thermodynamics. *arXiv preprint arXiv:1503.03585*, 2015.
- [51] Jiaming Song, Chenlin Meng, and Stefano Ermon. Denoising diffusion implicit models. *arXiv preprint arXiv:2010.02502*, 2020.
- [52] Yang Song and Stefano Ermon. Generative modeling by estimating gradients of the data distribution. In *Advances in Neural Information Processing Systems (NeurIPS)*, 2019.
- [53] Yang Song and Stefano Ermon. Improved techniques for training score-based generative models. *arXiv preprint arXiv:2006.09011*, 2020.
- [54] Yang Song and Diederik P Kingma. How to train your energy-based models. *arXiv preprint arXiv:2101.03288*, 2021.
- [55] Yang Song, Jascha Sohl-Dickstein, Diederik P Kingma, Abhishek Kumar, Stefano Ermon, and Ben Poole. Score-based generative modeling through stochastic differential equations. In *International Conference on Learning Representations (ICLR)*, 2021.
- [56] Charles Stein et al. A bound for the error in the normal approximation to the distribution of a sum of dependent random variables. In *Proceedings of the Sixth Berkeley Symposium on Mathematical Statistics and Probability, Volume 2: Probability Theory*. The Regents of the University of California, 1972.
- [57] Omer Tov, Yuval Alaluf, Yotam Nitzan, Or Patashnik, and Daniel Cohen-Or. Designing an encoder for stylegan image manipulation. *ACM Transactions on Graphics (TOG)*, 40(4):1–14, 2021.
- [58] Pascal Vincent. A connection between score matching and denoising autoencoders. *Neural computation*, 23(7):1661–1674, 2011.
- [59] Ting-Chun Wang, Ming-Yu Liu, Jun-Yan Zhu, Andrew Tao, Jan Kautz, and Bryan Catanzaro. High-resolution image synthesis and semantic manipulation with conditional gans. In *IEEE Conference on Computer Vision and Pattern Recognition (CVPR)*, 2018.
- [60] Zongze Wu, Dani Lischinski, and Eli Shechtman. Stylespace analysis: Disentangled controls for stylegan image genera-

- tion. In *Proceedings of the IEEE/CVF Conference on Computer Vision and Pattern Recognition*, 2021.
- [61] Wenqi Xian, Patsorn Sangkloy, Varun Agrawal, Amit Raj, Jingwan Lu, Chen Fang, Fisher Yu, and James Hays. Texturegan: Controlling deep image synthesis with texture patches. In *IEEE Conference on Computer Vision and Pattern Recognition (CVPR)*, 2018.
 - [62] Jianwen Xie, Yang Lu, Ruiqi Gao, and Ying Nian Wu. Cooperative learning of energy-based model and latent variable model via mcmc teaching. In *Proceedings of the AAAI Conference on Artificial Intelligence*, volume 32, 2018.
 - [63] Jianwen Xie, Yang Lu, Song-Chun Zhu, and Yingnian Wu. A theory of generative convnet. In *International Conference on Machine Learning*, pages 2635–2644. PMLR, 2016.
 - [64] Yinghao Xu, Yujun Shen, Jiapeng Zhu, Ceyuan Yang, and Bolei Zhou. Generative hierarchical features from synthesizing images. In *Proceedings of the IEEE/CVF Conference on Computer Vision and Pattern Recognition*, pages 4432–4442, 2021.
 - [65] Chao Yang, Xin Lu, Zhe Lin, Eli Shechtman, Oliver Wang, and Hao Li. High-resolution image inpainting using multi-scale neural patch synthesis. In *IEEE Conference on Computer Vision and Pattern Recognition (CVPR)*, 2017.
 - [66] Hang Zhang, Kristin Dana, Jianping Shi, Zhongyue Zhang, Xiaogang Wang, Amrith Tyagi, and Amit Agrawal. Context encoding for semantic segmentation. In *Proceedings of the IEEE conference on Computer Vision and Pattern Recognition*, pages 7151–7160, 2018.
 - [67] Richard Zhang, Phillip Isola, and Alexei A Efros. Colorful image colorization. In *European Conference on Computer Vision (ECCV)*, 2016.
 - [68] Richard Zhang, Jun-Yan Zhu, Phillip Isola, Xinyang Geng, Angela S Lin, Tianhe Yu, and Alexei A Efros. Real-time user-guided image colorization with learned deep priors. *ACM Transactions on Graphics (TOG)*, 9(4), 2017.
 - [69] Yang Zhou, Zhen Zhu, Xiang Bai, Dani Lischinski, Daniel Cohen-Or, and Hui Huang. Non-stationary texture synthesis by adversarial expansion. *ACM Transactions on Graphics (TOG)*, 37(4), 2018.
 - [70] Jiapeng Zhu, Yujun Shen, Deli Zhao, and Bolei Zhou. In-domain gan inversion for real image editing. In *European Conference on Computer Vision (ECCV)*, 2020.
 - [71] Jun-Yan Zhu, Philipp Krähenbühl, Eli Shechtman, and Alexei A Efros. Generative visual manipulation on the natural image manifold. In *European Conference on Computer Vision (ECCV)*, 2016.
 - [72] Jun-Yan Zhu, Taesung Park, Phillip Isola, and Alexei A Efros. Unpaired image-to-image translation using cycle-consistent adversarial networks. In *IEEE International Conference on Computer Vision (ICCV)*, 2017.
 - [73] Peihao Zhu, Rameen Abdal, Yipeng Qin, and Peter Wonka. Sean: Image synthesis with semantic region-adaptive normalization. In *IEEE Conference on Computer Vision and Pattern Recognition (CVPR)*, 2020.

A. Implementation Details

Below, we add additional implementation details for each application. Our code and models will be publicly available upon publication.

Stroke-based image synthesis. In this experiment, we use $N = 500$, $t_0 = 0.5$, for SDEdit (VP); and $N = 1000$, $t_0 = 0.45$ for SDEdit (VE). We find that $K = 1$ to 3 work reasonably well, with larger K generating more realistic images but at a higher computational cost.

For both StyleGAN2-ADA and in-domain GAN, we use the official implementation with default parameters to project each input image into the latent space, and subsequently use the obtained latent code to produce stroke-based image samples.

Stroke-based image editing. We use $K = 1$ in the experiment for SDEdit (VP). We use $t_0 = 0.5$, $N = 500$ for SDEdit (VP), and $t_0 = 0.45$, $N = 1000$ for SDEdit (VE).

Image compositing. We use CelebA-HQ (256×256) [29] for image compositing experiments. More specifically, given an image from CelebA-HQ, the user will copy pixel patches from other reference images, and also specify the pixels they want to perform modifications. In general, the masks are simply the pixels the users have copied pixel patches to. We focus on editing hairstyles and adding glasses. We use an SDEdit model pretrained on FFHQ [31] or CelebA-HQ [29]. We use $t_0 = 0.3$, $N = 300$, $K = 3$ for SDEdit (VP), and $t_0 = 0.35$, $N = 700$, $K = 3$ for SDEdit (VE). We present more results in Appendix B.2.

B. Extra experimental results

B.1. Extra results on LSUN datasets

Stroke-based image generation. We present more SDEdit (VP) results on LSUN bedroom in Figure 7. We use $t_0 = 0.5$, $N = 500$, and $K = 2$. We observe that, SDEdit is able to generate realistic images that share the same structure as the input paintings when *no paired data is provided*.

Stroke-based image editing. We present more SDEdit (VP) results on LSUN bedroom in Figure 8. SDEdit generates image edits that are both realistic and faithful to the user edit, while avoids making undesired modifications on pixels not specified by users. See Appendix A for experimental settings.

B.2. Extra results on CelebA-HQ datasets

Stroke-based image editing. We provide intermediate step visualizations for SDEdit (VP) in Figure 9. We present

extra SDEdit (VP) results on CelebA-HQ in Figure 10. We also presents results on CelebA-HQ (1024×1024) in Fig. 15. SDEdit generates images that are both realistic and faithful (to the user edit), while avoids introducing undesired modifications on pixels not specified by users. We provide experiment settings in Appendix A.

Image compositing. We focus on editing hair styles and adding glasses. We present more SDEdit (VP) results on CelebA-HQ (256×256) in Figure 11, Figure 12, and Figure 13. We also presents results on CelebA-HQ (1024×1024) in Figure 14. We observe that SDEdit can generate both faithful and realistic edited images. See Appendix A for experiment settings.

C. Details on the VE and VP SDEs

We follow the definitions of VE and VP SDEs in [55], and adopt the same settings therein. In particular, for the VE SDE, we choose

$$\sigma(t) = \begin{cases} 0, & t = 0 \\ \sigma_{\min} \left(\frac{\sigma_{\max}}{\sigma_{\min}} \right)^t, & t > 0 \end{cases}$$

where $\sigma_{\min} = 0.01$ and $\sigma_{\max} = 380, 378, 348, 1348$ for LSUN churches, bedroom, FFHQ/CelebA-HQ 256 × 256, and FFHQ 1024 × 1024 datasets respectively.

For the VP SDE, it takes the form of

$$d\mathbf{x}(t) = -\frac{1}{2}\beta(t)\mathbf{x}(t)dt + \sqrt{\beta(t)}d\mathbf{w}(t), \quad (5)$$

where $\beta(t)$ is a positive function. In experiments, we follow [55, 23] and set

$$\beta(t) = \beta_{\min} + t(\beta_{\max} - \beta_{\min}),$$

where $\beta_{\min} = 0.1$ and $\beta_{\max} = 20$ across all datasets. We always have $p_1(\mathbf{x}) \approx \mathcal{N}(\mathbf{0}, \mathbf{I})$ under these settings.

Solving the reverse VP SDE is similar to solving the reverse VE SDE. Specifically, we follow the iteration rule below:

$$\mathbf{x}_{n-1} = \frac{1}{\sqrt{1 - \beta(t_n)\Delta t}}(\mathbf{x}_n + \beta(t_n)\Delta t \mathbf{s}_{\theta}(\mathbf{x}(t_n), t_n)) + \sqrt{\beta(t_n)\Delta t} \mathbf{z}_n, \quad (6)$$

where $\mathbf{x}_N \sim \mathcal{N}(\mathbf{0}, \mathbf{I})$, $\mathbf{z}_n \sim \mathcal{N}(\mathbf{0}, \mathbf{I})$ and $n = N, N-1, \dots, 1$.

D. Details on Stochastic Differential Editing

In this section, we present the algorithm for SDEdit (VP) on stroke-based image synthesis in Algorithm 3. We present

the algorithm for the general flexible image editing method in Algorithm 4.

Algorithm 3 Stroke-based image synthesis with SDEdit (VP SDE)

Require: \mathbf{x} (stroke painting), t_0 (SDE hyper-parameter), N (total denoising steps), K (total repeats)

$$\Delta t \leftarrow \frac{t_0}{N}$$

$$\alpha(t_0) \leftarrow \prod_{n=1}^N (1 - \beta(\frac{nt_0}{N})\Delta t)$$

for $k \leftarrow 1$ **to** K **do**

$$\mathbf{z} \sim \mathcal{N}(\mathbf{0}, \mathbf{I})$$

$$\mathbf{x} \leftarrow \sqrt{\alpha(t_0)}\mathbf{x} + \sqrt{1 - \alpha(t_0)}\mathbf{z}$$

for $n \leftarrow N$ **to** 1 **do**

$$t \leftarrow t_0 \frac{n}{N}$$

$$\mathbf{z} \sim \mathcal{N}(\mathbf{0}, \mathbf{I})$$

$$\mathbf{x} \leftarrow \frac{1}{\sqrt{1 - \beta(t)\Delta t}}(\mathbf{x} + \beta(t)\Delta t \mathbf{s}_\theta(\mathbf{x}, t)) + \sqrt{\beta(t)\Delta t} \mathbf{z}$$

end for

end for

Return \mathbf{x}

Algorithm 4 Stochastic Differential Editing (VP SDE)

Require: \mathbf{x} (source image), Ω (mask for edited regions), t_0 (SDE hyper-parameter), N (total denoising steps), K (total repeats)

$$\Delta t \leftarrow \frac{t_0}{N}$$

$$\mathbf{x}_0 \leftarrow \mathbf{x}$$

$$\alpha(t_0) \leftarrow \prod_{i=1}^N (1 - \beta(\frac{it_0}{N})\Delta t)$$

for $k \leftarrow 1$ **to** K **do**

$$\mathbf{z} \sim \mathcal{N}(\mathbf{0}, \mathbf{I})$$

$$\mathbf{x} \leftarrow [(1 - \Omega) \odot \sqrt{\alpha(t_0)}\mathbf{x}_0 + \Omega \odot \sqrt{\alpha(t_0)}\mathbf{x} + \sqrt{1 - \alpha(t_0)}\mathbf{z}]$$

for $n \leftarrow N$ **to** 1 **do**

$$t \leftarrow t_0 \frac{n}{N}$$

$$\mathbf{z} \sim \mathcal{N}(\mathbf{0}, \mathbf{I})$$

$$\alpha(t) \leftarrow \prod_{i=1}^n (1 - \beta(\frac{it_0}{N})\Delta t)$$

$$\mathbf{x} \leftarrow \left\{ (1 - \Omega) \odot (\sqrt{\alpha(t)}\mathbf{x}_0 + \sqrt{1 - \alpha(t)}\mathbf{z}) + \Omega \odot \left[\frac{1}{\sqrt{1 - \beta(t)\Delta t}}(\mathbf{x} + \beta(t)\Delta t \mathbf{s}_\theta(\mathbf{x}, t)) + \sqrt{\beta(t)\Delta t} \mathbf{z} \right] \right\}$$

end for

end for

Return \mathbf{x}



Figure 7: Stroke-based image generation on bedroom images with SDEdit (VP) pretrained on LSUN bedroom.

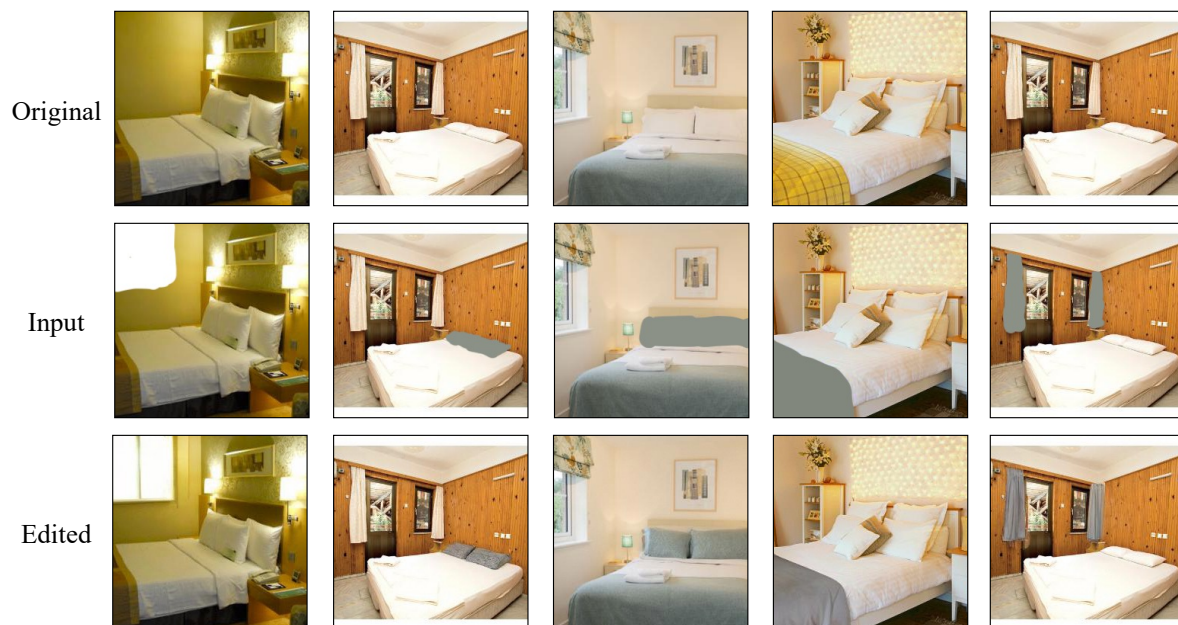


Figure 8: Stroke-based image editing on bedroom images with SDEdit (VP) pretrained on LSUN bedroom. SDEdit generates image edits that are both realistic and faithful (to the user edit), while avoids making undesired modifications on pixels not specified by users

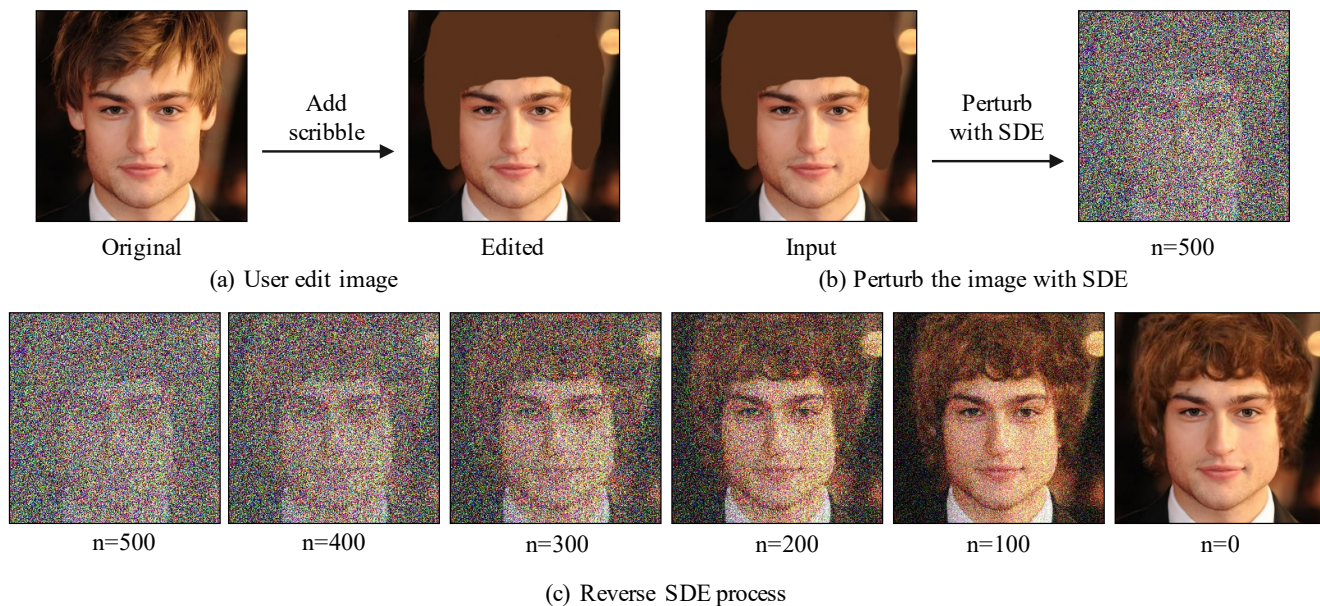


Figure 9: Stroke-based image editing. Given an image, users will first modify the image using stroke, and provide a mask which describes the pixels covered by stroke (see Figure (a)) . The edited image will then be fed into SDEdit. SDEdit will first perturb the image with an SDE (see Figure (b)), and then simulate the reverse SDE (see Algorithm 4). We provide visualization of the intermediate steps of reversing SDE used in SDEdit (see Figure (c)).



Figure 10: Stroke-based image editing on CelebA-HQ images with SDEdit (VP). SDEdit generates image edits that are both realistic and faithful (to the user edit), while avoids making undesired modifications on pixels not specified by users.



Figure 11: Image compositing on CelebA-HQ images with SDEdit (VP). We edit the images to have brown hair. The model is pretrained on FFHQ.



Figure 12: Image compositing on CelebA-HQ images with SDEdit (VP). We edit the images to wear glasses. The model is pretrained on FFHQ.



Figure 13: Image compositing on CelebA-HQ images with SDEdit (VP). We edit the images to have blond hair. The model is pretrained on FFHQ.

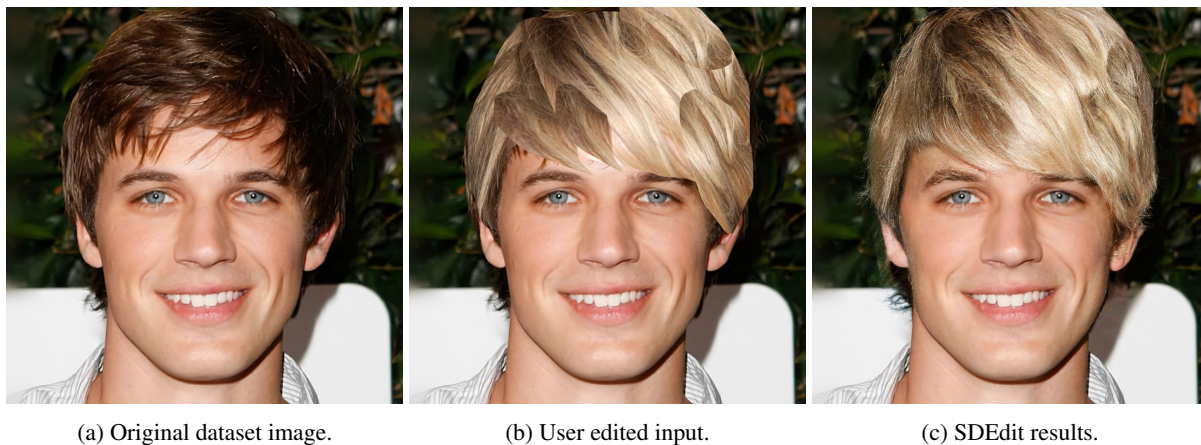


Figure 14: Image compositing results with SDEdit (VE) on CelebA-HQ (resolution 1024×1024). The SDE model is pre-trained on FFHQ.

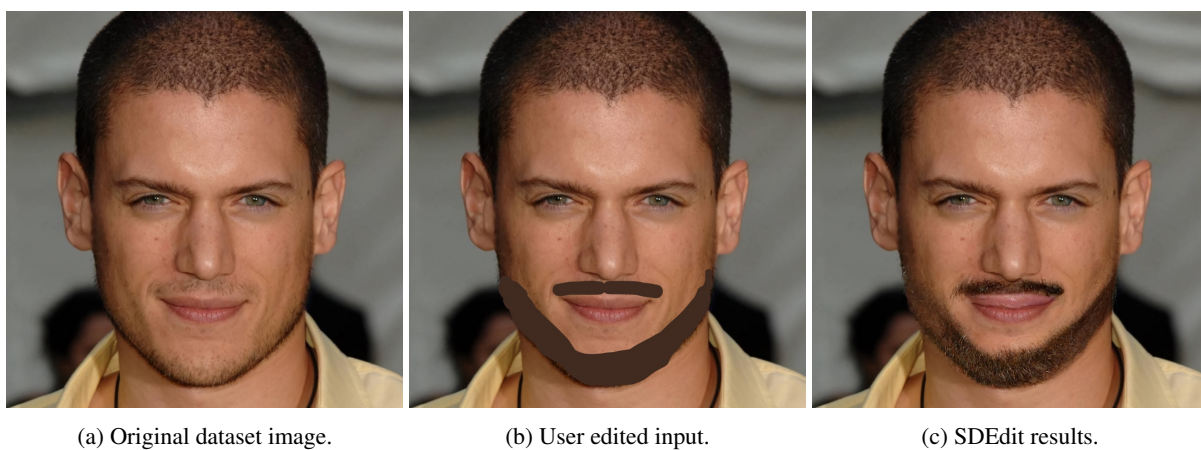


Figure 15: Stroke-based image editing results with SDEdit (VE) on CelebA-HQ (resolution 1024×1024). The SDE model is pretrained on FFHQ.